BUCKLING ANALYSIS OF FUNCTIONALLY GRADED MINDLIN PLATES SUBJECTED TO LINEARLY VARYING IN-PLANE LOADING USING POWER SERIES METHOD OF FROBENIUS

M. Bodaghi

Department of Mechanical Engineering, Shahid Bahonar University of Kerman, Kerman, Iran
mahdibodaghi@gmail.com

A.R. Saidi *

Department of Mechanical Engineering, Shahid Bahonar University of Kerman, Kerman, Iran
saidi@mail.uk.ac.ir

*Corresponding Author

(Received: August 02, 2011 – Accepted in Revised Form: December 15, 2011)

doi: *10.5829/idosi.ije.2012.25.01a.09*

Abstract In this paper, buckling behavior of moderately thick functionally graded rectangular plates resting on elastic foundation subjected to linearly varying in-plane loading is investigated. The neutral surface position for a functionally graded plate which its material properties vary in the thickness direction is determined. Based on the first-order shear deformation plate theory and the neutral surface concept, the equilibrium and stability equations are derived. An analytical approach is employed to decouple the stability equations, as these equations are converted into two decoupled equations. Employing Levy-type solution, the buckling equation is reduced to an ordinary differential equation with variable coefficients! and solved exactly using power series method of Frobenius. To examine accuracy of the present formulation and procedure, several convergence and comparison studies are investigated. Furthermore, the effects of different parameters of plate and elastic foundation on the critical buckling load of functionally graded rectangular plate are discussed.

Keywords Buckling analysis; Functionally graded material; Power series solution; Linear in-plane loading; Elastic foundation; Mindlin plate.

چکیده در این مقاله رفتار کمانشی ورق‌های مستطیلی ساخته شده از مواد هدفمند بر روی بستر الاستیک و تحت بارگذاری درون صفحه‌ای که به طور خطی تغییر می کند مورد بررسی قرار گرفته است. موقعیت رویه - ی خنثی برای ورق هدفمند که خواص آن در جهت ضخامتش تغییر می‌کند تعیین شده است. براساس تئوری تغییر شکل برشی مرتبه‌ی اول ورق و مفهوم صفحه‌ی خنثای فیزیکی، معادلات تعادل و پایداری به دست آمده است. به منظور جداسازی معادلات پایداری، یک روش تحلیلی به کار گرفته شده است به گونه‌ای که این معادلات به دو معادله‌ی مستقل تبدیل شده‌اند. با استفاده از روش حل لوی، معادله‌ی کمانش به یک معادله‌ی دیفرانسیل معمولی با ضرایب متغیر تبدیل و سپس به صورت دقیق با استفاده از روش سری توانی فروبنیوس حل شده است. به منظور بررسی دقت حل حاضر چند مطالعه مقایسه‌ای و همگرایی انجام شده است. همچنین تاثیر پارامترهای مختلف ورق و بستر الاستیک روی بار بحرانی کمانش ورق مستطیلی ساخته شده از مواد هدفمند مورد بررسی قرار گرفته است.

1. INTRODUCTION

The study on buckling of plate structures supported by an elastic foundation is one of the most important research areas in applied mechanics. Pasternak's two-parameter model [1] is commonly adopted to describe the mechanical behavior of foundations, and the well-known Winkler's model [2] is one of its special cases. Many researchers employed classical plate theory (CPT) to analyze buckling behavior of thin plates. For example, Lam et al. [3] studied the elastic bending, buckling and vibration problems of rectangular thin Levy-plates resting on elastic foundation. Buckling of

orthotropic rectangular thin plates subjected to uniaxial in-plane loading was analyzed by Harik and Balakrishnan [4]. Yu and Wang [5] presented an exact solution for buckling analysis of isotropic rectangular thin Levy-plates on one-parameter elastic foundation under different uniform loading conditions. Since the classical plate theory neglects the effects of transverse shear deformation plate, it underestimates the deflection and overestimates the natural frequencies and buckling loads of moderately thick and thick plates. To modify the classical plate theory for moderately thick plates, the first-order shear deformation theory (FSDT) was proposed by Mindlin and his co-workers [6, 7]. Brunelle [8] analyzed the elastic buckling of transversely isotropic Mindlin plates with two opposite edges simply supported and the remaining two edges subjected to various boundary conditions. Hosseini-Hashemi et al. [9] described an investigation on exact solution for linear buckling of rectangular Mindlin plates with two opposite edges simply supported. According to the literature survey, it can be found that most of the buckling studies have dealt with rectangular plates having uniformly distributed in-plane edge loads. This is due to the fact that the governing stability equations have constant coefficients which yield exact solutions for buckling loads when two opposite edges of the plate are simply supported. Certainly, a plate may be loaded at the supported edges by non-uniform in-plane loading. For instance, in the case of I-beam or wide flanged beam under bending moment at the ends or lateral loads on the flange, the web of the beam is subjected to non-uniform in-plane loads. In the past decade, some works have been published for static and dynamic analysis of rectangular plates under non-uniformly varying in-plane loading. For example, Romeo and Ferrero [10] investigated analytical/experimental behavior of symmetric laminated simply-supported and clamped rectangular panels under linearly varying combined loads. They indicated that there exists a good correlation between analytical, numerical and experimental results. Also, they believed that a slight initial imperfection in the plate geometry has a great effect on the discrepancy between theoretical and experimental results. Bert and Devarakonda [11] presented the buckling loads of a simply supported rectangular thin plate under sinusoidal distribution of in-plane loading using Galerkin method. In a series of articles, Leissa and Kang [12] and Kang and Leissa [13, 14] have used the classical plate theory and the power series method to give the exact solutions for vibration and buckling of the thin plate having two opposite edges simply supported subjected to linearly varying in-plane load. Liew and Chen [15] used the radial point interpolation method to investigate buckling of rectangular Mindlin plates subjected to partial in-plane edge loads. By using Galerkin's approach, Jana and Bhaskar [16] investigated buckling of a simply supported rectangular plate under various non-uniform compressive edge loads. Buckling analysis of simply supported symmetric cross-ply composite rectangular Mindlin plates under linearly varying edge loads was investigated by Zhong and Gu [17]. Lopatin and Morozov [18] presented the buckling solution for the *CCFF* orthotropic composite thin plates subjected to linearly distributed in-plane loads using the method of lines for partial differential equations and Galerkin's method. Panda and Ramachandra [19] presented the buckling load of a composite plate subjected to linearly and parabolically distributed in-plane loads by adopting Galerkin's approximation. The buckling behavior of moderately thick plates under linear in-plane loading was analyzed in a part of book prepared by Shanmugam and Wang [20]. Bodaghi and Saidi [21] investigated the stability analysis of standing laminated rectangular Mindlin plates subjected self-weight (or acceleration) and vertical loading.

Recent advances in material processing technology have led to a new class of materials called functionally graded materials (FGMs). Due to the advantages of being able to withstand severe high-temperature gradient while maintaining structural integrity, preliminary structural components, such as beams, plates and shells, made of FGMs have been increasingly applied in modern engineering and industry. Many researchers have analyzed the static and dynamic behavior of structural elements made of functionally graded materials [22- 26].

In the field of bucking analysis of FG plates, for example, Cheng and Kitipornchai [27] presented the exact explicit eigenvalues for compression buckling, hygrothermal buckling and vibration of

sandwich plates with dissimilar facings and functionally graded plates resting on elastic foundation via analogy with membrane vibration. Wu [28] investigated the thermal buckling analysis of a simply supported moderately thick rectangular FG plate based on the first-order shear deformation plate theory. Kazerouni et al. [29] presented thermal buckling analysis of thin functionally graded plates under two cases of thermal loadings as the uniform and non-linear temperature rise cases. Thermal buckling behavior of thick functionally graded rectangular plate was investigated by Bodaghi and Saidi [30] based on the Reddy's higher-order shear deformation plate theory. Mohammadi et al. [31] investigated the buckling analysis of moderately thick FG rectangular plates under uniform in-plane loading based on the FSDT.

Since, the material properties of functionally graded plate vary through the thickness direction, the neutral surface of such plate may not coincide with its geometric middle surface. Therefore, stretching and bending deformations of FG plate are coupled. Some researchers [32- 36] have shown that there is no stretching-bending coupling in constitutive equations if the reference surface is properly selected. Recently, Bodaghi and Saidi [37] investigated the buckling of thin FG plates under non-uniform in-plane loading in the framework of the classical thin plate theory. They used the neutral surface concept and showed that the stability equations based on the classical plate theory reduced to the single buckling equation which can be solved by using the power series method straightforwardly.

As mentioned earlier, the classical plate theory is not adequate in providing accurate buckling results when the thickness-to-length ratio of the plate is relatively large. The objective of this article is to obtain an exact analytical solution for buckling analysis of moderately thick shear deformable FG plates subjected to linear in-plane loading resting on elastic foundation. The present work is an extension of a previous authors' work [37] (which was valid for buckling analysis of thin FG plates) and uses the first-order shear deformation plate theory which provides accurate solution compared to the classical theory especially for moderately thick FGM plates.

The first-order theory based on the exact position of neutral surface together with principle of minimum total potential energy are employed to extract the equilibrium equations of the functionally graded rectangular plates resting on elastic foundation. By using the adjacent equilibrium criterion, the stability equations are obtained. Unlike the CPT which leads to the single stability equation [37], the FSDT results the three highly coupled stability equations which have been solved analytically in this paper. By definition of two new analytic functions the three coupled equations are reduced to two decoupled equations in term of transverse displacement and a new function called boundary layer function. By considering a functionally graded rectangular plate with two opposite simply supported edges and employing the Levy-type solution, the buckling equation is reduced to an ordinary differential equation with variable coefficients. This equation is exactly solved by the power series solution method of Frobenius. Imposing different boundary conditions along two other opposite edges of the FG plate, the critical buckling loads are obtained. Convergence study is first performed to evaluate the sufficiency of the proposed method for analyzing functionally graded plates under linear in-plane loading resting on elastic foundation with different boundary conditions. Then, the accuracy of the present results is verified through comparisons with the existing data reported in the literature. Moreover, the effects of plate parameters, power law index of FGM, foundation stiffness coefficients and loading factor together with various combinations of boundary conditions on the critical buckling load of Al/Al_2O_3 FG rectangular plate are discussed in detail.

2. PHYSICAL NEUTRAL SURFACE

FGMs are a special kind of composites in which their material properties vary smoothly and continuously due to gradually varying the volume fraction of the constituent materials along certain dimension (usually in the thickness direction). In this study, the FG plate is made from a mixture of ceramic and metal and the properties are assumed to vary through the thickness of the plate. Due to asymmetry of material properties of FG plates with

respect to middle plane, the stretching and bending equations are coupled. But, if the origin of the coordinate system is suitably selected in the thickness direction of the FG plate so as to be the neutral surface, the properties of the FG plate being symmetric with respect to it. To specify the position of neutral surface of FG plates, two different planes are considered for the measurement of z, namely, z_{ms} and z_{ns} measured from the middle surface and the neutral surface of the plate, respectively, as depicted in Figure 1.

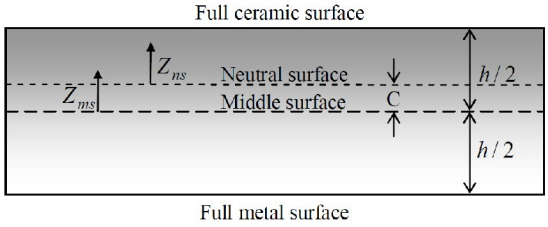

Figure 1. The positions of middle surface and neutral surface for FG plates

The volume-fraction of ceramic (V_c) can be expressed based on z_{ms} and z_{ns} coordinates as [38]

$$V_c = \left(\frac{z_{ms}}{h} + \frac{1}{2}\right)^p = \left(\frac{z_{ns} + C}{h} + \frac{1}{2}\right)^p \quad (1)$$

where h is the plate thickness and p denotes the power law index of FG plate $(p \geq 0)$ and the parameter C is the distance of neutral surface from the middle surface.

Since it is assumed that the FG plate is made from a mixture of ceramic and metal, the effective Young's modulus (E) based on the Voigt model [39] can be written as:

$$E(z) = E_m V_m(z) + E_c V_c(z) \quad (2)$$

in which the subscripts m and c represent the metallic and ceramic constituents, respectively. Also the volume fractions of metal and ceramic are related as follows [38]:

$$V_m(z) + V_c(z) = 1 \quad (3)$$

From Equations (2) and (3), the effective Young's modulus of FG plate can be rewritten as:

$$E(z) = E_m + (E_c - E_m) V_c(z) \quad (4)$$

The position of the neutral surface of the FG plate is determined to satisfy the first moment with respect to Young's modulus being zero as follows [34]:

$$\int_{-h/2}^{h/2} E(z_{ms})(z_{ms} - C) dz_{ms} = 0 \quad (5)$$

Consequently, the position of neutral surface is obtained as:

$$C = \frac{\int_{-h/2}^{h/2} E(z_{ms}) z_{ms} dz_{ms}}{\int_{-h/2}^{h/2} E(z_{ms}) dz_{ms}} \quad (6)$$

From Equation (6), it can be seen that the parameter C is zero for homogeneous isotropic plates, as expected.

3. GOVERNING EQUATIONS

A moderately thick FG rectangular plate with the length a, width b and uniform thickness h, resting on two-parameter elastic foundation is considered as depicted in Figure 2.

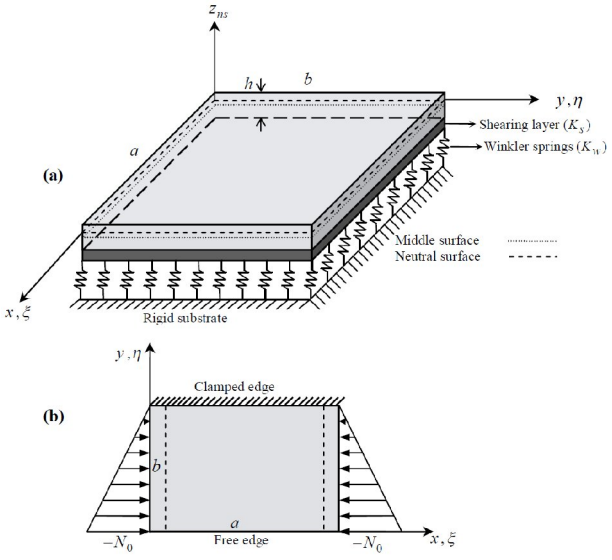

Figure 2. a) Configuration and coordinate system of a FG rectangular plate resting on elastic foundation, **b)** A *SFSC* plate under linearly varying in-plane loading

The origin of the Cartesian coordinate system is taken at the neutral surface of the FG plate. The FG plate having two opposite edges simply supported is subjected to linearly distributed in-plane loading at these two edges, while the remaining edges $(y = 0, b)$ may have any combinations of clamped, free or simply supported boundary conditions.

On the basis of the first-order shear deformation plate theory and physical neutral surface concept, the displacement components are assumed to be

$$\begin{aligned} U_1(x,y,z_{ns}) &= u(x,y) + z_{ns}\,\psi_x(x,y) \\ U_2(x,y,z_{ns}) &= v(x,y) + z_{ns}\,\psi_y(x,y) \\ U_3(x,y,z_{ns}) &= w(x,y) \end{aligned} \tag{7}$$

where (u,v,w) are the displacements of neutral surface of FG plate along the (x,y,z_{ns}) coordinate directions, respectively, and ψ_x and ψ_y denote the rotation functions. Substituting Equations (7) into von-Karman nonlinear strain-displacement relations [40], kinematic relations are obtained as:

$$\begin{aligned} \{\varepsilon\} &= \{\varepsilon^{(0)}\} + z_{ns}\{\varepsilon^{(1)}\} \\ \{\gamma\} &= \{\gamma^{(0)}\} \end{aligned} \tag{8}$$

where

$$\{\varepsilon\} = \begin{Bmatrix} \varepsilon_{xx} \\ \varepsilon_{yy} \\ \varepsilon_{xy} \end{Bmatrix}, \{\gamma\} = \begin{Bmatrix} \gamma_{xz} \\ \gamma_{yz} \end{Bmatrix}$$

$$\{\varepsilon^{(0)}\} = \begin{Bmatrix} u_{,x} + (w_{,x})^2/2 \\ v_{,y} + (w_{,y})^2/2 \\ u_{,y} + v_{,x} + w_{,x}w_{,y} \end{Bmatrix}, \{\varepsilon^{(1)}\} = \begin{Bmatrix} \psi_{x,x} \\ \psi_{y,y} \\ \psi_{x,y} + \psi_{y,x} \end{Bmatrix} \tag{9}$$

$$\{\gamma^{(0)}\} = \begin{Bmatrix} \psi_x + w_{,x} \\ \psi_y + w_{,y} \end{Bmatrix}$$

where a comma denotes partial differentiation with respect to the corresponding coordinate.

The linear constitutive relations for the plate in the plane stress state are given by [41]:

$$\{\sigma\} = [Q]\{\varepsilon\}, \{\tau\} = [\overline{Q}]\{\gamma\} \tag{10}$$

where

$$\{\sigma\} = \begin{Bmatrix} \sigma_{xx} \\ \sigma_{yy} \\ \sigma_{xy} \end{Bmatrix}, \{\tau\} = \begin{Bmatrix} \tau_{xz} \\ \tau_{yz} \end{Bmatrix} \tag{11}$$

$$[Q] = \frac{E(z)}{(1-\nu^2)} \begin{bmatrix} 1 & n & 0 \\ n & 1 & 0 \\ 0 & 0 & (1-n)/2 \end{bmatrix}, [\overline{Q}] = \frac{E(z)}{2(1+n)} \begin{bmatrix} 1 & 0 \\ 0 & 1 \end{bmatrix}$$

The parameter (ν) is the Poisson's ratio and since its variation through the thickness is relatively small, it is assumed to be constant [28-34].

According to the principle of minimum total potential energy [42], the equilibrium equations of the FG plate resting on two-parameter elastic foundation can be obtained as:

$$\begin{aligned} &N_{xx,x} + N_{xy,y} = 0 \\ &N_{xy,x} + N_{yy,y} = 0 \\ &M_{xx,x} + M_{xy,y} - Q_x = 0 \\ &M_{xy,x} + M_{yy,y} - Q_y = 0 \\ &Q_{x,x} + Q_{y,y} + N_{xx}w_{,xx} \\ &+ 2N_{xy}w_{,xy} + N_{yy}w_{,yy} - K_w w + K_s \nabla^2 w = 0 \end{aligned} \tag{12}$$

where ∇^2 is two-dimensional Laplace operator, and K_w and K_s are the transverse and shear stiffness coefficients of the elastic foundation, respectively. Also $N_i, M_i, (i = xx, yy, xy)$ are the resultant forces and moments, respectively, and $Q_i, (i = x, y)$ are the transverse shear forces which are all defined by the following expressions:

$$\begin{aligned} \{N\} &= \begin{Bmatrix} N_{xx} \\ N_{yy} \\ N_{xy} \end{Bmatrix} = \int_{-h/2-C}^{h/2-C} \{\sigma\} dz_{ns} \\ \{M\} &= \begin{Bmatrix} M_{xx} \\ M_{yy} \\ M_{xy} \end{Bmatrix} = \int_{-h/2-C}^{h/2-C} \{\sigma\} z_{ns} dz_{ns} \\ \{Q\} &= \begin{Bmatrix} Q_x \\ Q_y \end{Bmatrix} = K^2 \int_{-h/2-C}^{h/2-C} \{\tau\} dz_{ns} \end{aligned} \tag{13}$$

In Equation (13), K^2 is the shear correction factor which is assumed to be 5/6. By substituting Equation (8) into Equation (10) and the subsequent results into Equation (13), the stress resultants can be expressed in terms of displacements as follows:

$$\{N\}=[A]\{\varepsilon^{(0)}\},\{M\}=[D]\{\varepsilon^{(1)}\},\{Q\}=[C]\{\gamma^{(0)}\} \quad (14)$$

where

$$[A]=\int_{-h/2-C}^{h/2-C}[Q]\,dz_{ns}$$
$$[D]=\int_{-h/2-C}^{h/2-C}[Q]z_{ns}^2\,dz_{ns} \quad (15)$$
$$[C]=K^2\int_{-h/2-C}^{h/2-C}[\overline{Q}]\,dz_{ns}$$

In Equation (15), the matrices $[A]$, $[D]$ and $[C]$ are extensional, bending and transverse shear stiffness matrices, respectively. It may be noted that there is no extension-bending coupling matrix and stretching-bending coupling in the constitutive equations using the physical neutral surface concept.

To obtain the stability equations of the FG plate, the adjacent equilibrium criterion is employed [40]. Assume that the equilibrium state of a plate under in-plane loads is defined in terms of the displacement components u^0, v^0, w^0, ψ_x^0 and ψ_y^0. Consider an infinitesimally small increment from the stable configuration whose displacement components differ by u^1, v^1, w^1, ψ_x^1 and ψ_y^1 with respect to the equilibrium position. Thus, the total displacements of a neighboring configuration of the stable state can be written as follows:

$$u \to u^0+u^1\ ;\ v\to v^0+v^1\ ;\ w\to w^0+w^1$$
$$\psi_x\to\psi_x^0+\psi_x^1\ ;\ \psi_y\to\psi_y^0+\psi_y^1 \quad (16)$$

Substituting the relations (16) in Equations (14) yields:

$$\{N\}=\{N^{(0)}\}+\{N^{(1)}\}$$
$$\{M\}=\{M^{(0)}\}+\{M^{(1)}\} \quad (17)$$
$$\{Q\}=\{Q^{(0)}\}+\{Q^{(1)}\}$$

where the terms with superscripts 0 are corresponding to the equilibrium state and the terms with superscripts 1 are linear parts of the stress resultants increments corresponding to the neighboring state. By substituting Equations (16) and (17) into Equation (12), the terms in the resulting equation with superscript 0 satisfy the equilibrium condition and therefore omitted from the equations. Also, the nonlinear terms with superscript 1 are neglected because they are small compared to the linear terms [37]. The remaining terms form the stability equation of FG plate as:

$$N_{xx,x}^1+N_{xy,y}^1=0$$
$$N_{xy,x}^1+N_{yy,y}^1=0$$
$$M_{xx,x}^1+M_{xy,y}^1-Q_x^1=0 \quad (18)$$
$$M_{xy,x}^1+M_{yy,y}^1-Q_y^1=0$$
$$Q_{x,x}^1+Q_{y,y}^1+N_{xx}^0w_{,xx}^1+2N_{xy}^0w_{,xy}^1+N_{yy}^0w_{,yy}^1-K_ww^1+K_s\nabla^2w^1=0$$

where the parameters $N_i^0,(i=xx,yy,xy)$ denote the force resultants in the pre-buckling state.
By substituting the kinematic and constitutive relations into the stability Equation (18), the governing stability equations are obtained as

$$D_{11}\psi_{x,xx}^1+D_{12}\psi_{y,xy}^1+D_{33}(\psi_{x,yy}^1+\psi_{y,xy}^1)-C_{11}(\psi_x^1+w_{,x}^1)=0$$
$$D_{11}\psi_{y,yy}^1+D_{12}\psi_{x,xy}^1+D_{33}(\psi_{x,xy}^1+\psi_{y,xx}^1)-C_{22}(\psi_y^1+w_{,y}^1)=0$$
$$C_{11}(\psi_{x,x}^1+w_{,xx}^1)+C_{22}(\psi_{y,y}^1+w_{,yy}^1)$$
$$+N_{xx}^0w_{,xx}^1+2N_{xy}^0w_{,xy}^1+N_{yy}^0w_{,yy}^1-K_ww^1+K_s\nabla^2w^1=0 \quad (19)$$

These equations are three coupled partial differential equations in terms of rotation functions and transverse displacement. They may be solved by introducing the following auxiliary functions:

$$\varphi_1=\psi_{x,x}^1+\psi_{y,y}^1$$
$$\varphi_2=\psi_{x,y}^1-\psi_{y,x}^1 \quad (20)$$

Using above analytical functions and also by considering relations $D_{12}=D_{11}-2D_{33}$ and $C_{11}=C_{22}$, the governing stability Equation (19) are reduced to the following simpler form:

$$D_{11}\varphi_{1,x}+D_{33}\varphi_{2,y}-C_{11}(\psi_x^1+w_{,x}^1)=0 \quad (21a)$$

$$D_{11}\varphi_{1,y}-D_{33}\varphi_{2,x}-C_{11}(\psi_y^1+w_{,y}^1)=0 \quad (21b)$$

$$C_{11}(\varphi_1+\nabla^2w^1)+N_{xx}^0w_{,xx}^1+2N_{xy}^0w_{,xy}^1$$
$$+N_{yy}^0w_{,yy}^1-K_ww^1+K_s\nabla^2w^1=0 \quad (21c)$$

From Equation (21c), the function φ_1 can be written in terms of w^1 as:

$$\varphi_1=\frac{-1}{C_{11}}(N_{xx}^0w_{,xx}^1+2N_{xy}^0w_{,xy}^1+N_{yy}^0w_{,yy}^1$$
$$-K_ww^1+K_s\nabla^2w^1)-\nabla^2w^1 \quad (22)$$

By differentiation of Equations (21a) and (21b) with respect to x and y, respectively, and adding the results, the following equation can be obtained:

$$D_{11}\nabla^2\varphi_1 - C_{11}(\varphi_1 + \nabla^2 w^1) = 0 \qquad (23)$$

Substituting Equation (22) into Equation (23), yields:

$$\begin{aligned}&\frac{-D_{11}}{C_{11}}\nabla^2(N^0_{xx}w^1_{,xx} + 2N^0_{xy}w^1_{,xy} + N^0_{yy}w^1_{,yy} - K_w w^1\\ &+K_s\nabla^2 w^1) - D_{11}\nabla^4 w^1 + (N^0_{xx}w^1_{,xx} + N^0_{xy}w^1_{,xy}\\ &+N^0_{yy}w^1_{,yy} - K_w w^1 + K_s\nabla^2 w^1) = 0\end{aligned} \qquad (24)$$

Similarly, subtraction of the differentiation of Equation (21a) with respect to y and Equation (21b) with respect to x, it is concluded that:

$$D_{33}\nabla^2\varphi_2 - C_{11}\varphi_2 = 0 \qquad (25)$$

Therefore, three coupled governing stability Equations (21) are converted into two independent Equations (24) and (25). Equation (25) is known as the edge-zone (or boundary layer) equation of the plate, and the function φ_2 is referred to the boundary layer function.

Furthermore, by using Equations (21a), (21b) and (22), the rotation functions ψ^1_x and ψ^1_y can be expressed in terms of w^1 and φ_2 as follows:

$$\begin{aligned}\psi^1_x &= -(D_{11}/C^2_{11})((C_{11}+K_s)\nabla^2 w^1 + (C^2_{11}/D_{11} - K_w)w^1\\ &+N^0_{xx}w^1_{,xx} + 2N^0_{xy}w^1_{,xy} + N^0_{yy}w^1_{,yy})_{,x} + (D_{33}/C_{11})\phi_{2,y}\end{aligned} \qquad (26)$$

$$\begin{aligned}\psi^1_y &= -(D_{11}/C^2_{11})((C_{11}+K_s)\nabla^2 w^1 + (C^2_{11}/D_{11} - K_w)w^1\\ &+N^0_{xx}w^1_{,xx} + 2N^0_{xy}w^1_{,xy} + N^0_{yy}w^1_{,yy})_{,y} - (D_{33}/C_{11})\phi_{2,x}\end{aligned}$$

4. STABILITY ANALYSIS

4.1. Mechanical Loading As shown in Figure 2, the FG plate subjected to linearly varying in-plane loading acting on two opposite edges simply supported in y direction is considered.

The pre-buckling forces can be obtained using the equilibrium conditions as:

$$N^0_{xx} = -N_0(1-\alpha(y/b)) \ , \ N^0_{yy} = N^0_{xy} = 0 \qquad (27)$$

where N_0 and α are the intensity of the compressive force per unit length and a loading factor, respectively. By changing the factor α, various particular cases for linear in-plane loading may be obtained. For instance, if α is set to zero, the uniformly distributed compressive load is obtained. By taking various values of α in the range $0 < \alpha < 2$, an eccentric bending is obtained, which is a combination of pure bending and uniform compression. Examples of these cases are depicted in Figure 3.

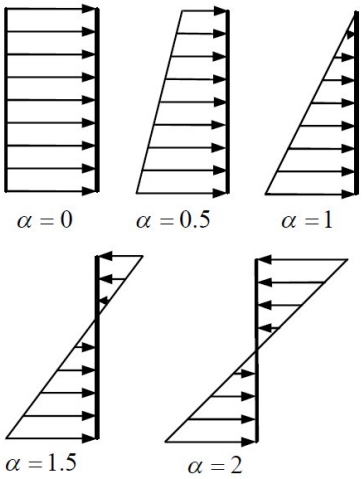

Figure 3. Examples of in-plane loading $N_{xx} = -N_0(1-\alpha\eta)$ along the edge $x = 0$

It may be noted that the case of $\alpha < 0$ or $\alpha > 2$ are not considered because such cases are identical with the cases of $0 < \alpha < 2$ as far as the edge conditions are the same.

By substituting the pre-buckling forces given in Equation (27) into the stability Equation (24), the buckling equation is obtained as follows:

$$\begin{aligned}&D_{11}\nabla^4 w^1 - \frac{D_{11}}{C_{11}}\nabla^2(K_w w^1 - K_s\nabla^2 w^1\\ &+ N_0(1-\alpha(y/b))w^1_{,xx}) + (K_w w^1 - K_s\nabla^2 w^1\\ &+ N_0(1-\alpha(y/b))w^1_{,xx}) = 0\end{aligned} \qquad (28)$$

Introducing the dimensionless coordinates $\xi = x/a$ and $\eta = y/b$, the buckling Equation (28) can be rewritten in the dimensionless form as:

$$
\begin{aligned}
&k^4(1+D_1\hat{K}_s)\hat{w}_{,\eta\eta\eta\eta}\\
&+(2k^2(1+D_1\hat{K}_s)-D_1N^*k^2(1-\alpha\eta))\hat{w}_{,\xi\xi\eta\eta}\\
&+((1+D_1\hat{K}_s)-D_1N^*(1-\alpha\eta))\hat{w}_{,\xi\xi\xi\xi}\\
&+(2D_1N^*k^2\alpha)\hat{w}_{,\xi\xi\eta}\\
&+(N^*(1-\alpha\eta)-(D_1\hat{K}_w+\hat{K}_s))\hat{w}_{,\xi\xi}\\
&-k^2(D_1\hat{K}_w+\hat{K}_s)\hat{w}_{,\eta\eta}+\hat{K}_w\hat{w}=0
\end{aligned}
\tag{29}
$$

where $k=a/b$ is the aspect ratio of the plate. Also, $\hat{K}_w,\hat{K}_s,N^*,D_1$ and $\hat{w}$ are the dimensionless parameters which are given as follows:

$$
\begin{aligned}
&\hat{K}_w=K_wa^4/D_{11}\\
&\hat{K}_s=K_sa^2/D_{11}\\
&N^*=N_0a^2/D_{11}\\
&D_1=D_{11}/C_{11}a^2\quad;\hat{w}=w^1/h
\end{aligned}
\tag{30}
$$

Furthermore, the boundary layer Equation (25) and equations of the rotation functions (26) in dimensionless form can rewritten as follows:

$$\hat{\varphi}_{2,\xi\xi}+k^2\hat{\varphi}_{2,\eta\eta}-\hat{\varphi}_2/D_3=0 \tag{31a}$$

$$
\begin{aligned}
&\hat{\psi}_x=-(D_1^2\delta)((\hat{K}_s+1/D_1)(\hat{w}_{,\xi\xi}+k^2\hat{w}_{,\eta\eta})\\
&-(\hat{K}_w-1/D_1^2)\hat{w}-N^*(1-\alpha\eta)\hat{w}_{,\xi\xi})_{,\xi}+D_3k\hat{\varphi}_{2,\eta}
\end{aligned}
\tag{31b}
$$

$$
\begin{aligned}
&\hat{\psi}_y=-(D_1^2k\delta)((\hat{K}_s+1/D_1)(\hat{w}_{,\xi\xi}+k^2\hat{w}_{,\eta\eta})\\
&-(\hat{K}_w-1/D_1^2)\hat{w}-N^*(1-\alpha\eta)\hat{w}_{,\xi\xi})_{,\eta}-D_3\hat{\varphi}_{2,\xi}
\end{aligned}
\tag{31c}
$$

where the dimensionless parameters $\hat{\varphi}_2, D_3$ and δ are defined as $a\varphi_2$, $D_3=D_{33}/C_{11}a^2$ and h/a respectively. It should be noted that rotation functions have dimensionless form.

4.2. Solution Methodology For a rectangular plate with simply supported edges at $\xi=0$ and 1, the Levy-type solution procedure may be used to solve the decoupled governing Equations (29) and (31a). The transverse displacement and boundary layer function can be assumed to be:

$$\hat{w}(\xi,\eta)=\sum_{m=1}^{\infty}T_m(\eta)\sin(m\pi\xi) \tag{32}$$

$$\hat{\varphi}_2(\xi,\eta)=\sum_{m=1}^{\infty}\Phi_m(\eta)\cos(m\pi\xi) \tag{33}$$

where m denotes the number of half-waves in the ξ direction. It is seen that Equations (32) and (33) exactly satisfy the simply supported boundary conditions at $\xi=0$ and $\xi=1$. Substituting the proposed series solution (32) into Equation (29) yields the following ordinary differential equation as:

$$
\begin{aligned}
&L_1T_m^{(4)}+(L_2+L_3\eta)T_m^{(2)}\\
&+2L_3T_m^{(1)}+(L_4+L_5\eta)T_m=0
\end{aligned}
\tag{34}
$$

where $T_m^{(4)}$, $T_m^{(2)}$ and $T_m^{(1)}$ are the fourth, second and first derivatives of T_m with respect to η, respectively. Also, the parameters $L_i\,(i=1..5)$ are defined as follows:

$$
\begin{aligned}
&L_1=k^4(1+D_1\hat{K}_s)\\
&L_2=-(k^2(\hat{K}_wD_1+\hat{K}_s)\\
&+(m\pi)^2[2k^2(\hat{K}_sD_1+1)-N^*D_1k^2])\\
&L_3=-N^*D_1k^2\alpha(m\pi)^2\\
&L_4=(m\pi)^4[(\hat{K}_sD_1+1)-N^*D_1]\\
&+(m\pi)^2[(\hat{K}_wD_1+\hat{K}_s)-N^*]+\hat{K}_w\\
&L_5=N^*\alpha(m\pi)^2(D_1(m\pi)^2+1)
\end{aligned}
\tag{35}
$$

Equation (34) is an ordinary differential equation with variable coefficients. To solve this equation the power series solution method of Frobenius [43] is used. To this end, the function $T_m(\eta)$ is written as:

$$T_m(\eta)=\sum_{n=0}^{\infty}C_{m,n}\,\eta^n \tag{36}$$

where $C_{m,n}$'s are arbitrary constant coefficients. Substitution of Equation (36) into Equation (34) yields:

$$
\begin{aligned}
&L_1\sum_{n=4}^{\infty}n(n-1)(n-2)(n-3)C_{m,n}\eta^{n-4}\\
&+L_2\sum_{n=2}^{\infty}n(n-1)C_{m,n}\eta^{n-2}\\
&+L_3(\sum_{n=2}^{\infty}n(n-1)C_{m,n}\eta^{n-1}+2\sum_{n=1}^{\infty}nC_{m,n}\eta^{n-1})\\
&+L_4\sum_{n=0}^{\infty}C_{m,n}\eta^n+L_5\sum_{n=0}^{\infty}C_{m,n}\eta^{n+1}=0
\end{aligned}
\tag{37}
$$

Shifting indices, Equation (37) becomes:

$$\begin{aligned} &L_1\sum_{n=0}^{\infty}(n+4)(n+3)(n+2)(n+1)C_{m,n+4}\eta^n \\ &+L_2\sum_{n=0}^{\infty}(n+2)(n+1)C_{m,n+2}\eta^n \\ &+L_3(\sum_{n=1}^{\infty}(n+1)nC_{m,n+1}\eta^n+2\sum_{n=0}^{\infty}(n+1)C_{m,n+1}\eta^n) \\ &+L_4\sum_{n=0}^{\infty}C_{m,n}\eta^n+L_5\sum_{n=1}^{\infty}C_{m,n-1}\eta^n=0 \end{aligned} \quad (38)$$

After collecting the coefficients of similar powers of η in Equation (38), one obtains from η^0:

$$C_{m,4}=\frac{-1}{24L_1}(2L_2C_{m,2}+2L_3C_{m,1}+L_4C_{m,0}) \quad (39)$$

and the coefficient of $\eta^n\ (n=1,2,3,...)$ gives:

$$\begin{aligned} &C_{m,n+4}=-\{(n+2)(n+1)(L_2C_{m,n+2}+L_3C_{m,n+1}) \\ &+L_4C_{m,n}+L_5C_{m,n-1}\}/\{(n+4)(n+3)(n+2)(n+1)L_1\} \end{aligned} \quad (40)$$

Relations (39) and (40) are the recurrence formulas for $C_{m,n}$ when $n\geq 4$. Thus, $C_{m,0}, C_{m,1}, C_{m,2}$ and $C_{m,3}$ are arbitrary constant coefficients and the other coefficients $C_{m,n}$ for $n\geq 4$ are expressed in terms of them. To solve Equation (31a), substituting the proposed series solution (33) into Equation (31a) yields an ordinary differential equation, which its general solution is given by:

$$\Phi_m(\eta)=C_{m,-2}\sinh(\zeta\eta)+C_{m,-1}\cosh(\zeta\eta) \quad (41)$$

where

$$\zeta=\sqrt{(m\pi/k)^2+1/(D_3k^2)} \quad (42)$$

The boundary conditions at other two edges of the FG plate $(\eta=0,1)$ which may have any combinations of clamped, free or simply supported boundary conditions are obtained from the principle of minimum total potential energy in dimensionless form as:

$$\begin{aligned} &Clamped: && \hat{w}=\hat{\psi}_x=\hat{\psi}_y=0 \\ &Simply\,Supported: && \hat{w}=\hat{\psi}_x=\hat{M}_{yy}=0 \\ &Free: && \hat{M}_{yy}=\hat{M}_{xy}=\hat{Q}_y+k\delta\hat{K}_sD_1\hat{w}_{,\eta}=0 \end{aligned} \quad (43)$$

where:

$$\begin{aligned} \hat{M}_{yy}&=(1-2D_3/D_1)\hat{\psi}_{x,\xi}+k\hat{\psi}_{y,\eta} \\ \hat{M}_{xy}&=(D_3/D_1)(\hat{\psi}_{y,\xi}+k\hat{\psi}_{x,\eta}) \\ \hat{Q}_y&=\hat{\psi}_y+k\delta\hat{w}_{,\eta} \end{aligned} \quad (44)$$

4.3. Critical Buckling Load Parameter By applying different boundary conditions at two edges of the rectangular plate in ξ direction ($\eta=0$ and $\eta=1$) a set of homogenous algebraic equations is obtained in terms of the unknown constant parameters $C_{m,-2}, C_{m,-1}, C_{m,0}, C_{m,1}, C_{m,2}, C_{m,3}$, and the buckling load parameter N^* for each longitudinal half-wave number (m). For a nontrivial solution, the determinant of the sixth order coefficient matrix must be set to zero which results in the characteristic equation. Solving this equation, the buckling load parameters of the FG plate are calculated. The lowest value among all these N^*'s for each m is known as the critical buckling load parameter (N^*_{cr}) and the corresponding m indicates the number of half-waves in the x direction of critical buckling mode shape.

5. RESULTS AND DISSCUSION

In order to obtain the numerical results, an Al/Al_2O_3 functionally graded plate composed of Aluminum $(E_m=70GPa)$ and Alumina $(E_c=380GPa)$ is considered. The Poisson's ratio of the plate is assumed to be constant through the thickness and equal to 0.3.

5.1. Examination of Convergence The Exact solution for the function stated in Equation (36) is summation of an infinite series and the accuracy of the results depends on the number of terms which are considered in the power series solution. Based on the degree of accuracy requirement in numerical calculations, the upper limit of the summation is truncated at a finite number (N). In order to check the convergence rate of the power series solution of Equation (36), the critical buckling load parameter of a FG plate resting on elastic foundation with all nine possible

combinations of boundary conditions has been listed in Table 1. It is seen that for all of boundary conditions more than 24 terms is required to achieve the critical buckling load parameter accurately to six significant digits. Furthermore, it can be seen that increasing the edge constraints and also the number of half-waves in the buckling mode shape, more terms of the power series must be taken to represent the buckling behavior of plate properly for six digits convergence. The bold numbers in the table are those beyond which the sixth digit does not change as N increases. As more terms are considered, the critical buckling load parameters converge to their exact values.

The numerical results from the power series method which will be presented in the next sections are obtained by taking sufficient terms (N) to converge to the number of digits shown in the tables.

5.2. Comparison Studies To validate the present formulation and procedure, the present results are compared with those available in the literature for thin and moderately thick isotropic plates subjected to linear in-plane loading [14, 20] and also for moderately thick FG plates under uniform load [31]. In Table 2, the critical buckling moments obtained from present solution have been compared with those reported by Kang and Leissa [14] based on the classical plate theory. The homogonous isotropic thin plate $(p = 0, \delta = 0.001)$ is under pure in-plane bending and the critical buckling moment $M^*_{cr} = N^*_{cr}/(6k^2)$ defined by Kang and Leissa [14] has been presented. As this table shows, there is an excellent agreement between these results.

TABLE 1. Convergence test of the critical buckling load parameter (N^*_{cr}) for the FG plate under linear in-plane loading $(\alpha = 0.5)$ resting on two-parameter elastic foundation $(\hat{K}_w = 50, \hat{K}_s = 10,\ p = 5,\ k = 1, \delta = 0.1)$

N^a	Boundary conditions								
	SCSC $(m=2)$	*SCSS* $(m=2)$	*SSSC* $(m=2)$	*SSSS* $(m=1)$	*SCSF* $(m=1)$	*SSSF* $(m=1)$	*SFSC* $(m=1)$	*SFSS* $(m=1)$	*SFSF* $(m=1)$
16	5.84342	4.83581	2.13431	0.80119	3.96002	0.69900	8.50141	2.56955	1.49012
18	9.73108	8.94081	6.33176	2.09124	9.57822	2.04997	9.98014	10.8740	9.89880
20	33.8179	9.45890	7.89910	7.17480	20.5893	8.73811	18.3589	30.3992	20.7149
22	83.7911	30.6894	25.6709	60.5797	50.0981	30.7116	29.78	35.9036	31.3256
24	94.8569	73.7891	83.2844	80.0112	54.5049	48.4992	38.3715	**35.9038**	**31.3260**
26	99.9047	86.2300	92.7001	82.8100	54.5160	**48.4996**	**38.3716**	35.9038	31.3260
28	101.176	93.6621	92.6282	82.8109	54.5170	48.4996	38.3716	35.9038	31.3260
30	101.408	96.1020	92.6301	**82.8204**	**54.5171**	48.4996	38.3716	35.9038	31.3260
32	101.443	96.6462	92.6401	82.8204	54.5171	48.4996	38.3716	35.9038	31.3260
34	101.447	**96.6996**	**92.6411**	82.8204	54.5171	48.4996	38.3716	35.9038	31.3260
36	**101.448**[b]	96.6996	92.6411	82.8204	54.5171	48.4996	38.3716	35.9038	31.3260
38	101.448	96.6996	92.6411	82.8204	54.5171	48.4996	38.3716	35.9038	31.3260
40	101.448	96.6996	92.6411	82.8204	54.5171	48.4996	38.3716	35.9038	31.3260

[a] N =Total number of terms used in the power series solution.
[b] The critical buckling load parameters in bold indicate the best convergent values in each column with the least N.

TABLE 2. Comparison of the critical buckling moments of the isotropic rectangular plates under pure in-plane bending for $k = 2.3$

Power series method	Boundary conditions								
	SCSC	*SCSS*	*SCSF*	*SSSC*	*SSSS*	*SSSF*	*SFSC*	*SFSS*	*SFSF*
Ref. [14]	$65.12^{(5)}$	$65.12^{(5)}$	$65.11^{(5)}$	$40.06^{(4)}$	$39.83^{(3)}$	$39.75^{(1)}$	$3.925^{(1)}$	$1.994^{(1)}$	$1.610^{(1)}$
Present	$65.121^{(5)}$	$65.120^{(5)}$	$65.112^{(5)}$	$40.063^{(4)}$	$39.832^{(3)}$	$39.746^{(1)}$	$3.9254^{(1)}$	$1.9941^{(1)}$	$1.6101^{(1)}$

The superscript numbers within the parenthesis indicate number of half-waves in the x direction of critical buckling mode shape.

Another comparative study for evaluation of critical buckling loads between the presented solution and analytical solution developed by Mohammadi et al. [31] based on the FSDT, is performed in Table 3 for moderately thick FG plate without elastic foundation and subjected to uniform in-plane loading. From the results presented in Table 3, it is observed that results have a good agreement.

Furthermore, in Table 4, an interesting comparison study of the present exact power series solution with the extended Kantorovich method (EKM) published by Shanmugam and Wang [20] is shown for buckling analysis of moderately thick isotropic plate subjected to linearly distributed in-plane loading ($\alpha = 1,2$). This table indicates that our presented results are accurate. Finally, three comparative studies show that the results obtained from the proposed method agree well with existing analytical results in the literature which validate the reliability and accuracy of the present analytical approach.

5.3. Parametric Investigations In this section, to examine the effects of different parameters of plate and elastic foundation on the critical buckling load parameter a FG plate with all nine possible combinations of boundary conditions, the comprehensive results are tabulated in Tables 5 through 9.

In Table 5, the influence of aspect ratio on the critical buckling load parameters (N_{cr}^{*}) of a FG plate under linearly distributed in-plane loading resting on elastic foundation is investigated. It is observed that the critical buckling load increases by increasing the aspect ratio. This observation indicates that between two plates having identical length a, thickness h and boundary conditions, the one which has smaller width b buckles at greater in-plane loading. Also, the number of half-waves in the critical buckling mode shape (m), except for *SFSF* plates, increases with increasing the plate aspect ratio. Furthermore, the critical buckling load parameter of *SFSF* plate increases very slowly when the aspect ratio increases.

To examine the influence of foundation stiffness coefficients on the critical buckling load parameter, the values N_{cr}^{*} listed in Table 6 for the FG plate under linearly distributed in-plane loading resting on elastic foundation with various values of foundation stiffness coefficients; ($\hat{K}_w = 0,10,10^2,10^3, \hat{K}_s = 0,10,10^2$). As it can be seen, with increase of the foundation stiffness coefficients, critical buckling load parameter increases. Also, the results show that the shear stiffness coefficient ($\hat{K}_s$) has more effect on increasing the critical buckling load parameter than the transverse stiffness coefficient ($\hat{K}_w$). Table 7 shows the buckling behavior of the FG plate subjected to various linear in-plane loads. It can be seen that the critical buckling load parameter of the FG plate under linearly varying in-plane loading increases as the loading factor (α) increases for all boundary conditions. Also, it is seen that the critical buckling load parameters of FG plate with $\alpha = 2$ (pure in-plane bending) and clamped boundary condition at the edge $\eta = 0$ are almost identical for various boundary conditions at the other edge. This event can be partially described as the compressive loading in one half of the plate ($0 \le \eta \le 1/2$) destabilizes the FG plate while the tensile loading in the other half ($1/2 < \eta \le 1$) stabilizes it, with both effects virtually negating each other if the compression edge is clamped. When the boundary condition in edge $\eta = 0$ is simply supported, small differences can be observed between their critical buckling load parameters. For the remaining three cases, the results show that the critical buckling load of *SFSC* plate is greater than those of *SFSS* and *SFSF* plates while the critical buckling loads of these two plates are close to each other.

To gain a clear understanding of the buckling behavior of FG plates subjected to pure in-plane bending, the critical buckling mode shapes of the buckled plates related to the last row Table 7 are illustrated in Figures 4-6. From these figures, the results similar to those for critical buckling load parameters of FG plates with the same boundary condition in edge $\eta = 0$ examined above can be attained for the corresponding buckling mode shapes. Table 8 illustrates the influence of the thickness-side ratio on the critical buckling load parameters. It can be observed that, as the thickness-side ratio δ increases from 0.05 to 0.2, the critical buckling load parameter decreases. Such behavior is due to the effect of the transverse shear deformation in the FG plates.

TABLE 3. Comparison study of the critical buckling load (N_{cr}^*) for a FG plate under uniform in-plane loading $(\alpha = 0)$ versus the aspect ratio, thickness-side ratio and some power law indices

p	δ	k		Boundary conditions					
				SCSC	*SCSS*	*SSSS*	*SCSF*	*SSSF*	*SFSF*
1	0.1	0.5	Ref. [31]	18.174525$^{(1)}$	16.334756$^{(1)}$	14.982947$^{(1)}$	10.687864$^{(1)}$	10.450346$^{(1)}$	9.360683$^{(1)}$
			Present study	18.1745254$^{(1)}$	16.3347562$^{(1)}$	14.9829468$^{(1)}$	10.6878642$^{(1)}$	10.4503465$^{(1)}$	9.3606832$^{(1)}$
		1	Ref. [31]	64.819473$^{(2)}$	52.341359$^{(1)}$	37.713203$^{(1)}$	15.494974$^{(1)}$	13.322055$^{(1)}$	9.146917$^{(1)}$
			Present study	64.8194728$^{(2)}$	52.3413590$^{(1)}$	37.7132026$^{(1)}$	15.4949739$^{(1)}$	13.3220554$^{(1)}$	9.1469175$^{(1)}$
	0.2	0.5	Ref. [31]	16.204868$^{(1)}$	14.850333$^{(1)}$	13.805765$^{(1)}$	9.915186$^{(1)}$	9.728321$^{(1)}$	8.750235$^{(1)}$
			Present study	16.2048682$^{(1)}$	14.8503335$^{(1)}$	13.8057653$^{(1)}$	9.9151861$^{(1)}$	9.7283215$^{(1)}$	8.7502355$^{(1)}$
		1	Ref. [31]	46.134692$^{(2)}$	42.929636$^{(1)}$	33.252680$^{(1)}$	13.905245$^{(1)}$	12.251502$^{(1)}$	8.548311$^{(1)}$
			Present study	46.1346916$^{(2)}$	42.9296360$^{(1)}$	33.2526797$^{(1)}$	13.9052453$^{(1)}$	12.2515016$^{(1)}$	8.54834110$^{(1)}$
2	0.1	0.5	Ref. [31]	18.172610$^{(1)}$	16.333362$^{(1)}$	14.981870$^{(1)}$	10.687136$^{(1)}$	10.449673$^{(1)}$	9.360119$^{(1)}$
			Present study	18.1726101$^{(1)}$	16.3333621$^{(1)}$	14.9818697$^{(1)}$	10.6871362$^{(1)}$	10.4496731$^{(1)}$	9.3601190$^{(1)}$
		1	Ref. [31]	64.796315$^{(2)}$	52.331428$^{(1)}$	37.708938$^{(1)}$	15.493342$^{(1)}$	13.321007$^{(1)}$	9.146357$^{(1)}$
			Present study	64.7963151$^{(2)}$	52.3314284$^{(1)}$	37.7089377$^{(1)}$	15.4933425$^{(1)}$	13.3210071$^{(1)}$	9.1463570$^{(1)}$
	0.2	0.5	Ref. [31]	16.199079$^{(1)}$	14.845829$^{(1)}$	13.802108$^{(1)}$	9.912818$^{(1)}$	9.726090$^{(1)}$	8.748334$^{(1)}$
			Present study	16.990787$^{(1)}$	14.8458288$^{(1)}$	13.8021080$^{(1)}$	9.9128177$^{(1)}$	9.7260898$^{(1)}$	8.7483337$^{(1)}$
		1	Ref. [31]	46.091205$^{(2)}$	42.904167$^{(1)}$	33.239421$^{(1)}$	13.900689$^{(1)}$	12.248297$^{(1)}$	8.546461$^{(1)}$
			Present study	46.092052$^{(2)}$	42.9041673$^{(1)}$	33.2394207$^{(1)}$	13.9006890$^{(1)}$	12.2482972$^{(1)}$	8.5464612$^{(1)}$

The superscript numbers within the parenthesis indicate number of half-waves in the x direction of critical buckling mode shape.

TABLE 4. Comparison of the critical buckling load parameters (N_{cr}^*/π^2) for an isotropic rectangular plate under two case of in-plane loading versus thickness-side ratio $(k = 1)$

Boundary conditions	α	Method	Thickness-side ratio (δ)				
			0.01	0.05	0.1	0.15	0.2
SCSC	1	EKM [20]	14.6798$^{(2)}$	13.9548$^{(2)}$	12.1526$^{(2)}$	10.0708$^{(2)}$	8.1695$^{(2)}$
		Power series	14.67981$^{(2)}$	13.95485$^{(2)}$	12.15264$^{(2)}$	10.07076$^{(2)}$	8.16952$^{(2)}$
	2	EKM [20]	39.5131$^{(2)}$	36.2903$^{(2)}$	29.1478$^{(3)}$	20.8065$^{(3)}$	14.1835$^{(4)}$
		Power series	39.51308$^{(2)}$	36.29028$^{(2)}$	29.14777$^{(3)}$	20.80652$^{(3)}$	14.18352$^{(4)}$
SSSS	1	EKM [20]	7.8076$^{(1)}$	7.7045$^{(1)}$	7.3991$^{(1)}$	6.9402$^{(1)}$	6.3852$^{(1)}$
		Power series	7.80760$^{(1)}$	7.70452$^{(1)}$	7.39913$^{(1)}$	6.94023$^{(1)}$	6.38520$^{(1)}$
	2	EKM [20]	25.4793$^{(2)}$	24.3571$^{(2)}$	21.4086$^{(2)}$	17.8109$^{(2)}$	14.4145$^{(2)}$
		Power series	25.47933$^{(2)}$	24.35709$^{(2)}$	21.40858$^{(2)}$	17.81087$^{(2)}$	14.41453$^{(2)}$
SFSF	1	EKM [20]	1.6394$^{(1)}$	1.6208$^{(1)}$	1.5791$^{(1)}$	1.5201$^{(1)}$	1.4477$^{(1)}$
		Power series	1.63944$^{(1)}$	1.62081$^{(1)}$	1.57907$^{(1)}$	1.52006$^{(1)}$	1.44774$^{(1)}$
	2	EKM [20]	2.5990$^{(1)}$	2.5509$^{(1)}$	2.4606$^{(1)}$	2.3437$^{(1)}$	2.2086$^{(1)}$
		Power series	2.59904$^{(1)}$	2.55091$^{(1)}$	2.46056$^{(1)}$	2.34366$^{(1)}$	2.20856$^{(1)}$

The superscript numbers within the parenthesis indicate number of half-waves in the x direction of critical buckling mode shape.

TABLE 5. The critical buckling load parameter (N_{cr}^{*}) for a FG plate subjected to linearly varying in-plane loading $(\alpha = 0.5)$ versus aspect ratio $(\hat{K}_w = 10, \hat{K}_s = 10, p = 1, \delta = 0.1)$

Boundary conditions	Aspect ratio (k)								
	0.5	0.75	1	1.5	2	2.5	3	3.5	4
SCSC	42.3345$^{(1)}$	71.7162$^{(1)}$	102.7856$^{(2)}$	180.6462$^{(3)}$	253.4071$^{(3)}$	323.9195$^{(4)}$	386.1915$^{(5)}$	438.5575$^{(6)}$	481.5189$^{(7)}$
SCSS	40.5790$^{(1)}$	62.5507$^{(1)}$	97.5648$^{(2)}$	157.4859$^{(2)}$	232.4162$^{(3)}$	306.5035$^{(4)}$	372.2600$^{(5)}$	427.5665$^{(6)}$	472.8451$^{(7)}$
SSSC	38.7217$^{(1)}$	58.9585$^{(1)}$	93.2960$^{(2)}$	149.4060$^{(2)}$	223.0771$^{(3)}$	296.9714$^{(4)}$	363.2950$^{(5)}$	419.5265$^{(6)}$	465.8450$^{(7)}$
SSSS	37.4873$^{(1)}$	52.8294$^{(1)}$	77.9607$^{(1)}$	132.3264$^{(2)}$	203.1645$^{(2)}$	270.9240$^{(3)}$	341.1030$^{(4)}$	404.0789$^{(5)}$	457.1058$^{(6)}$
SCSF	34.5019$^{(1)}$	40.3791$^{(1)}$	48.3260$^{(1)}$	74.8770$^{(1)}$	112.1929$^{(2)}$	139.5282$^{(2)}$	176.6506$^{(2)}$	223.2620$^{(3)}$	256.9603$^{(3)}$
SSSF	33.4223$^{(1)}$	37.4545$^{(1)}$	42.3924$^{(1)}$	56.0324$^{(1)}$	74.8880$^{(1)}$	98.8737$^{(1)}$	127.8430$^{(1)}$	150.8473$^{(2)}$	174.0650$^{(2)}$
SFSC	25.5523$^{(1)}$	28.8277$^{(1)}$	33.9671$^{(1)}$	51.6480$^{(1)}$	78.1938$^{(2)}$	96.5891$^{(2)}$	121.8398$^{(2)}$	155.3187$^{(2)}$	179.4091$^{(3)}$
SFSS	25.4215$^{(1)}$	27.9432$^{(1)}$	31.3596$^{(1)}$	41.0113$^{(1)}$	54.4449$^{(1)}$	71.5703$^{(1)}$	92.2746$^{(1)}$	109.0040$^{(2)}$	125.5919$^{(2)}$
SFSF	25.0375$^{(1)}$	25.9154$^{(1)}$	26.2940$^{(1)}$	26.5001$^{(1)}$	26.5123$^{(1)}$	26.6709$^{(1)}$	26.7791$^{(1)}$	26.8126$^{(1)}$	26.9209$^{(1)}$

The superscript numbers within the parenthesis indicate number of half-waves in the x direction of critical buckling mode shape.

TABLE 6. The critical buckling load parameter (N_{cr}^{*}) of a FG plate under linearly varying in-plane loading $(\alpha = 1)$ with different foundation stiffness coefficients $(p = 2, k = 0.5, \delta = 0.1)$

$(\hat{K}_w, \hat{K}_s)$	Boundary conditions								
	SCSC	*SCSS*	*SSSC*	*SSSS*	*SCSF*	*SSSF*	*SFSC*	*SFSS*	*SFSF*
(0,0)	34.6057$^{(1)}$	33.2153$^{(1)}$	28.6522$^{(1)}$	27.7958$^{(1)}$	31.1923$^{(1)}$	26.7246$^{(1)}$	13.5030$^{(1)}$	13.4018$^{(1)}$	13.3488$^{(1)}$
(0,10)	58.0782$^{(1)}$	57.0457$^{(1)}$	50.5137$^{(1)}$	49.8652$^{(1)}$	55.7391$^{(1)}$	49.0025$^{(1)}$	27.4521$^{(1)}$	27.4035$^{(1)}$	27.2747$^{(1)}$
(0,10^2)	234.3193$^{(2)}$	234.2898$^{(2)}$	226.2815$^{(2)}$	226.2797$^{(2)}$	234.3382$^{(2)}$	226.2770$^{(2)}$	151.3134$^{(1)}$	151.2586$^{(1)}$	150.9459$^{(1)}$
(10,0)	36.4445$^{(1)}$	35.1548$^{(1)}$	30.3477$^{(1)}$	29.5547$^{(1)}$	33.4734$^{(1)}$	28.6607$^{(1)}$	14.7239$^{(1)}$	14.6931$^{(1)}$	13.7893$^{(1)}$
(10,10)	59.8546$^{(1)}$	58.8257$^{(1)}$	52.1721$^{(1)}$	51.5586$^{(1)}$	57.4192$^{(1)}$	50.7874$^{(1)}$	28.6825$^{(1)}$	28.6337$^{(1)}$	28.6156$^{(1)}$
(10,10^2)	234.6862$^{(2)}$	234.6657$^{(2)}$	226.6284$^{(2)}$	226.6266$^{(2)}$	234.7733$^{(2)}$	226.6240$^{(2)}$	152.5549$^{(1)}$	152.5133$^{(1)}$	152.4563$^{(1)}$
(10^2,0)	52.7147$^{(1)}$	51.8906$^{(1)}$	45.2669$^{(1)}$	44.8601$^{(1)}$	51.4142$^{(1)}$	44.6775$^{(1)}$	25.7136$^{(1)}$	25.7473$^{(1)}$	25.7118$^{(1)}$
(10^2,10)	75.6958$^{(1)}$	75.0840$^{(1)}$	66.8602$^{(1)}$	66.4857$^{(1)}$	74.6704$^{(1)}$	66.1994$^{(1)}$	39.7455$^{(1)}$	39.7195$^{(1)}$	39.5897$^{(1)}$
(10^2,10^2)	237.8939$^{(2)}$	237.8907$^{(2)}$	229.7474$^{(2)}$	229.7458$^{(2)}$	237.9165$^{(2)}$	229.7434$^{(2)}$	163.6643$^{(1)}$	163.6318$^{(1)}$	163.5931$^{(1)}$
(10^3,0)	107.4560$^{(2)}$	107.4374$^{(2)}$	101.4387$^{(2)}$	101.4378$^{(2)}$	107.4209$^{(2)}$	101.4375$^{(2)}$	72.1988$^{(2)}$	72.2002$^{(2)}$	72.2237$^{(2)}$
(10^3,10)	123.8482$^{(2)}$	123.6805$^{(2)}$	117.3961$^{(2)}$	117.3953$^{(2)}$	123.8268$^{(2)}$	117.3950$^{(2)}$	84.6247$^{(2)}$	84.6242$^{(2)}$	84.6242$^{(2)}$
(10^3,10^2)	269.7107$^{(2)}$	269.7011$^{(2)}$	260.6861$^{(2)}$	260.6854$^{(2)}$	269.6803$^{(2)}$	260.6846$^{(2)}$	194.9369$^{(2)}$	194.9369$^{(2)}$	194.9369$^{(2)}$

The superscript numbers within the parenthesis indicate number of half-waves in the x direction of critical buckling mode shape.

TABLE 7. Effect of loading factor on critical buckling load parameter (N_{cr}^{*}) for a FG plate subjected to uniformly and linearly distributed in-plane compressive loading $(\hat{K}_w = 100, \hat{K}_s = 0, p = 0.5, k = 1.5, \delta = 0.1)$

loading factors	Boundary conditions								
	SCSC	*SCSS*	*SSSC*	*SSSS*	*SCSF*	*SFSC*	*SSSF*	*SFSS*	*SFSF*
$\alpha = 0$	$121.1445^{(2)}$	$100.8810^{(2)}$	$100.8810^{(2)}$	$85.8430^{(2)}$	$36.3951^{(1)}$	$36.3951^{(1)}$	$28.1686^{(1)}$	$28.1686^{(1)}$	$19.224^{(1)}$
$\alpha = 0.5$	$160.8305^{(2)}$	$137.6310^{(2)}$	$130.3370^{(2)}$	$113.8509^{(2)}$	$59.9910^{(1)}$	$40.6281^{(1)}$	$44.7237^{(1)}$	$32.2241^{(1)}$	$24.9585^{(1)}$
$\alpha = 1$	$229.9634^{(3)}$	$209.7952^{(2)}$	$180.2759^{(2)}$	$164.1895^{(2)}$	$159.6855^{(1)}$	$45.8369^{(1)}$	$101.3876^{(1)}$	$37.4356^{(1)}$	$32.9467^{(1)}$
$\alpha = 1.5$	$342.0180^{(3)}$	$340.6393^{(3)}$	$271.7698^{(2)}$	$261.5581^{(2)}$	$340.2203^{(3)}$	$52.3357^{(1)}$	$258.4898^{(2)}$	$44.2398^{(1)}$	$42.3120^{(1)}$
$\alpha = 2$	$479.7145^{(4)}$	$479.7095^{(4)}$	$405.9504^{(3)}$	$405.8373^{(3)}$	$479.7045^{(4)}$	$60.5449^{(1)}$	$405.7710^{(3)}$	$53.2037^{(1)}$	$52.6261^{(1)}$

The superscript numbers within the parenthesis indicate number of half-waves in the x direction of critical buckling mode shape.

TABLE 8. The critical buckling load parameter (N_{cr}^{*}) for a FG plate subjected to linearly varying in-plane loading $(\alpha = 1.5)$ versus thickness-side ratio $(\hat{K}_w = 100, \hat{K}_s = 10, p = 3, k = 0.75)$

(δ)	Boundary conditions								
	SCSC	*SCSS*	*SCSF*	*SSSC*	*SSSS*	*SSSF*	*SFSC*	*SFSS*	*SFSF*
0.05	$179.8404^{(2)}$	$179.79021^{(2)}$	$179.3265^{(2)}$	$149.9898^{(2)}$	$149.7905^{(2)}$	$149.7367^{(2)}$	$50.6290^{(1)}$	$50.2124^{(1)}$	$50.1723^{(1)}$
0.1	$160.1752^{(2)}$	$160.1316^{(2)}$	$160.1248^{(2)}$	$138.4178^{(2)}$	$138.3878^{(2)}$	$138.3827^{(2)}$	$50.0345^{(1)}$	$49.8511^{(1)}$	$49.8117^{(1)}$
0.15	$137.8269^{(2)}$	$137.8008^{(2)}$	$137.7940^{(2)}$	$123.4697^{(2)}$	$123.4501^{(2)}$	$123.4448^{(2)}$	$49.2442^{(1)}$	$49.0834^{(1)}$	$49.0433^{(1)}$
0.2	$117.0808^{(2)}$	$117.0651^{(2)}$	$117.0603^{(2)}$	$108.1495^{(2)}$	$108.1374^{(2)}$	$108.1327^{(2)}$	$48.2926^{(1)}$	$48.1556^{(1)}$	$48.1153^{(1)}$

The superscript numbers within the parenthesis indicate number of half-waves in the x direction of critical buckling mode shape.

TABLE 9. The critical buckling load parameter $(N^{*} = N_0 a^2 / D_{11C})$ for a FG plate under pure in-plane bending $(\alpha = 2)$ versus various power law indices $(\hat{K}_w = 10, \hat{K}_s = 10, k = 1, \delta = 0.1)$

Boundary conditions	Power law index						
	0	0.5	1	2	5	10	100
SCSC	$310.9380^{(3)}$	$208.7411^{(3)}$	$163.0953^{(3)}$	$126.8068^{(3)}$	$101.4103^{(3)}$	$88.7699^{(3)}$	$62.7729^{(3)}$
SCSS	$310.9377^{(3)}$	$208.7409^{(3)}$	$163.0951^{(3)}$	$126.8066^{(3)}$	$101.4100^{(3)}$	$88.7696^{(3)}$	$62.7728^{(3)}$
SCSF	$310.9371^{(3)}$	$208.7405^{(3)}$	$163.0948^{(3)}$	$126.8064^{(3)}$	$101.4098^{(3)}$	$88.7695^{(3)}$	$62.7727^{(3)}$
SSSC	$247.7828^{(2)}$	$163.2372^{(2)}$	$126.4293^{(2)}$	$98.4943^{(2)}$	$81.1775^{(2)}$	$72.5548^{(2)}$	$50.6296^{(2)}$
SSSS	$247.7453^{(2)}$	$163.2130^{(2)}$	$126.4108^{(2)}$	$98.4798^{(2)}$	$81.1651^{(2)}$	$72.5435^{2)}$	$50.6218^{(2)}$
SSSF	$247.7201^{(2)}$	$163.1961^{(2)}$	$126.3975^{(2)}$	$98.4695^{(2)}$	$81.1569^{(2)}$	$72.5363^{(2)}$	$50.6167^{(2)}$
SFSC	$51.6420^{(1)}$	$33.5672^{(1)}$	$25.8417^{(1)}$	$20.1592^{(1)}$	$16.9745^{(1)}$	$15.4126^{(1)}$	$10.6465^{(1)}$
SFSS	$50.5186^{(1)}$	$32.8293^{(1)}$	$25.2709^{(1)}$	$19.7144^{(1)}$	$16.6064^{(1)}$	$15.0822^{(1)}$	$10.4166^{(1)}$
SFSF	$50.2949^{(1)}$	$32.6853^{(1)}$	$25.1606^{(1)}$	$19.6282^{(1)}$	$16.5327^{(1)}$	$15.0146^{(1)}$	$10.3702^{(1)}$

The superscript numbers within the parenthesis indicate number of half-waves in the x direction of critical buckling mode shape.

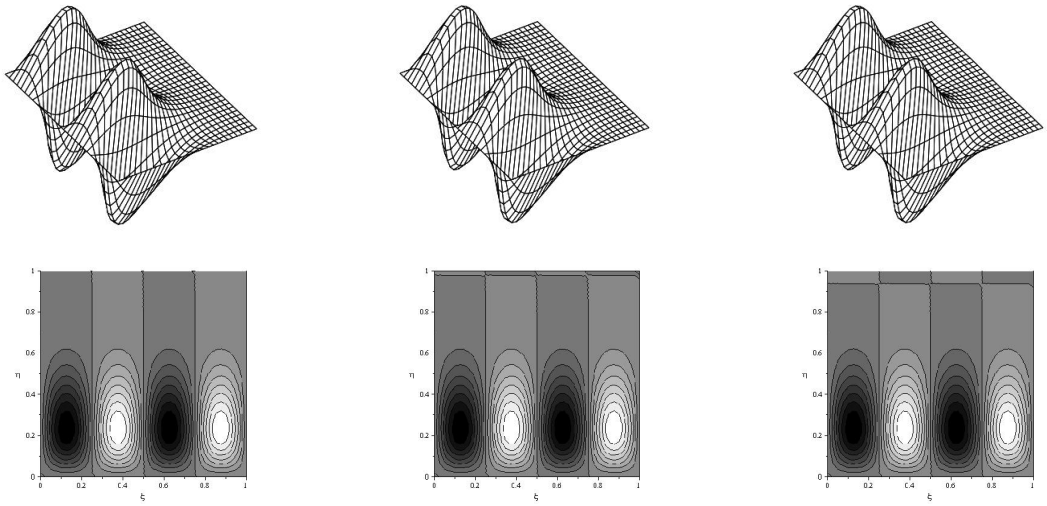

$SCSC, N_{cr}^{*} = 479.7145^{(4)}$ $SCSS, N_{cr}^{*} = 479.7095^{(4)}$ $SCSF, N_{cr}^{*} = 479.7045^{(4)}$

Figure 4. The critical buckling mode shapes of the FG plates pure in-plane bending and clamped boundary condition at the edge $\eta = 0$

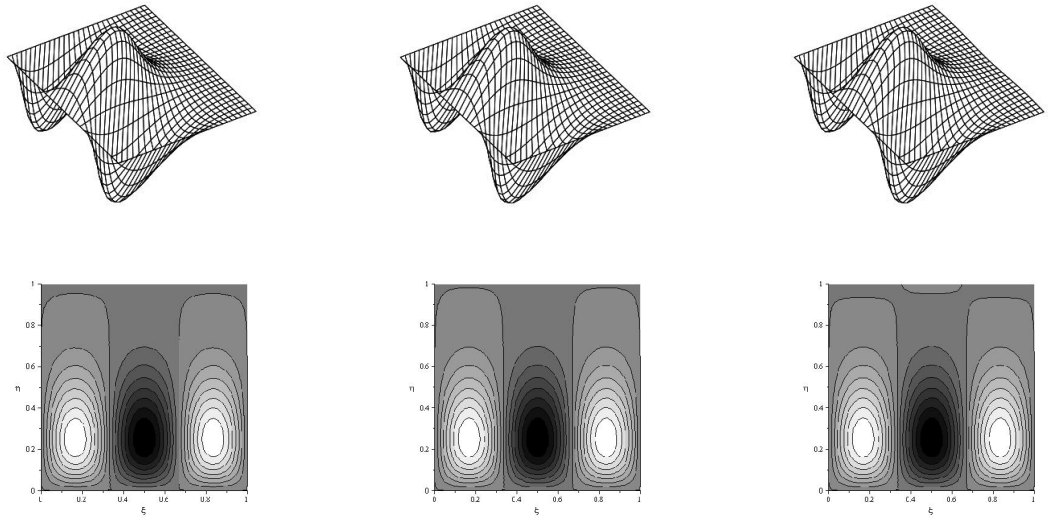

$SSSC, N_{cr}^{*} = 405.9504^{(3)}$ $SSSS, N_{cr}^{*} = 405.8373^{(3)}$ $SSSF\ N_{cr}^{*} = 405.7710^{(3)}$

Figure 5. The critical buckling mode shapes of the FG plates pure in-plane bending and simply supported boundary condition at the edge $\eta = 0$

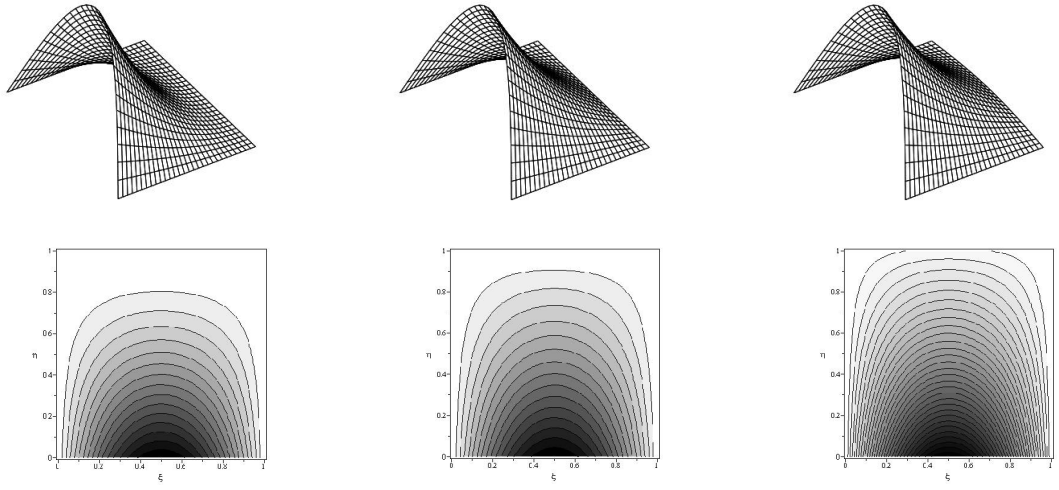

$SFSC, N_{cr}^{*} = 60.5449^{(1)}$ $SFSS, N_{cr}^{*} = 53.2037^{(1)}$ $SFSF, N_{cr}^{*} = 52.6261^{(1)}$

Figure 6. The critical buckling mode shapes of the FG plates pure in-plane bending and free boundary condition at the edge $\eta = 0$

To investigate the effect of power law index on the critical buckling load parameter, the values of $N_0 a^2 / D_{11c}$ (D_{11c} denotes the parameter D_{11} of FG plate when power law index is equal to zero) are presented in Table 9. It is observed that with the increase of power law index the critical buckling load parameter decreases. This is due to the fact that increasing the power law index increases the volume fraction of metal.

Finally, in order to gain a better understanding of the location of the neutral surface, the variation of dimensionless parameter C/h is illustrated in Figure 7 versus the power law index. It can be found that the dimensionless parameter C/h increases with increasing p and reaches maximum value of 0.15795 for $p = 3.3$, then the curve drops down and approaches zero asymptotically. Also, it can be seen that when the power law index becomes zero (pure ceramic plate) or infinity (pure metallic plate); the neutral surface coincides on the middle surface, as expected.

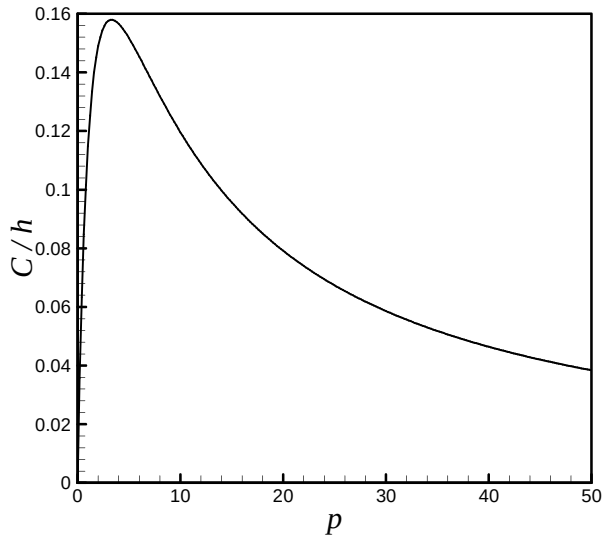

Figure 7. Variation of the neutral surface position versus power law index

6. CONCLUSION

In the present study, buckling behavior of functionally graded rectangular plates subjected to linearly varying in-plane loading acting on two opposite simply supported edges has been investigated on the basis of the first-order shear deformation plate theory. By using the principle of minimum total potential energy, the equilibrium equations of the FG plate resting on two-parameter elastic foundation have been derived. Introducing two auxiliary functions and carrying out some algebraic manipulations, the coupled stability partial differential equations have been decoupled. Then, considering Levy-type solution procedure, the buckling equation has been reduced to an ordinary differential equation with variable coefficients and solved using power series method of Frobenius. After appropriate convergence study, to ensure the accuracy of the derived formulations, the results obtained by the present solution have been compared with those reported in the literature. A good correlation has been observed between the present results and the available data in literature. Several parametric studies have been performed to show the effects of aspect ratio, foundation stiffness coefficients, plate thickness, in-plane loading condition and also power law index on the critical buckling load parameter of functionally graded rectangular plate with different boundary conditions. Finally, some general conclusions can be drawn as follows:

1) Good correlation can be seen between the buckling results of present power series solution and existing results from other analytical solutions.

2) By increasing the edge constraints and also the number of half-waves in the buckling mode shape, more terms of the power series solution are needed to represent the buckling behavior of FG plate properly.

3) The critical buckling load increases by increasing the aspect ratio. However, it decreases when the thickness-side ratio increases.

4) By increasing the power law index, the critical buckling load parameters normalized by D_{11c}, decreases.

5) The shear stiffness coefficient $(\hat{K}_s)$ exerts a greater influence on the critical buckling load parameter compared to the normal stiffness coefficient $(\hat{K}_w)$.

6) The critical buckling load parameter of the FG plate under linearly varying in-plane loading increases as the loading factor (α) increases for all boundary conditions.

7) The critical buckling load parameters for the case of FG plate under pure in-plane bending $(\alpha = 2)$ are almost identical when the compression side of the FG plate is clamped.

7. REFERENCES

1. Pasternak, P.L., "On a new method of analysis of an elastic foundation by means of two foundation constants", (1954), 1-56.
2. Winkler, E., Die Lehre von der Elasticitaet und Festigkeit, Prag, Dominicus, (1867).
3. Lam, K.Y., Wang, C.M. and He, X.Q., "Canonical exact solutions for levy-plates on two-coefficient foundation using green's functions", ***Engineering Structures***, Vol. 22, (2000), 364-378.
4. Harik, I.E. and Balakrishnan, N., "Stability of orthotropic rectangular plates", ***Applied Mathematical Modelling***, Vol. 18, (1994), 400-402.
5. Yu, L.H. and Wang, C.Y., "Buckling of rectangular plates on an elastic foundation using the levy solution", ***Journal of AIAA***, Vol. 46, (2008), 3163-3166.
6. Mindlin, R.D., "Influence of rotary inertia and shear in flexural motion of isotropic elastic plates", ***Journal of Applied Mechanics-ASME***, Vol. 18, (1951), 31-38.
7. Mindlin, R.D., Schaknow, A. and Deresiewicz, H., "Flexural vibration of rectangular plates", ***Journal of Applied Mechanics-ASME***, Vol. 23, (1956), 430-436.
8. Brunelle, E.J., "Buckling of transversely isotropic Mindlin plates", ***Journal of AIAA***, Vol. 19, (1971), 1018-1022.
9. Hosseini-Hashemi, S., Khorshidi, K. and Amabili, M., "Exact solution for linear buckling of rectangular Mindlin plates", ***Journal of Sound and Vibration***, Vol. 315, (2008), 318-342.
10. Romeo, G. and Ferrero, G., "Analytical/experimental behavior of anisotropic rectangular panels under linearly varying combined loads", ***Journal of AIAA***, Vol. 39, (2001), 932-941.
11. Bert, C.W. and Devarakonda, K.K., "Buckling of rectangular plates subjected to nonlinearly distributed in-plane loading", ***International Journal of Solids and Structures***, Vol. 40, (2003), 4097-4106.
12. Leissa, A.W. and Kang, J.H., "Exact solutions for vibration and buckling of an SS-C-SS-C rectangular plate loaded by linearly varying in-plane stresses", ***International Journal of Mechanical Sciences***, Vol. 44, (2002), 1925-1945.
13. Kang, J.H. and Leissa, A.W., "Vibration and buckling of SS-F-SS-F rectangular plates loaded by in-plane moments", ***International Journal of Structural stabilityand Dynamics***, Vol. 1, (2001), 527-543.
14. Kang, J.H. and Leissa, A.W., "Exact solutions for the buckling of rectangular plates having linearly varying

in-plane loading on two opposite simply supported edges", ***International Journal of Solids and Structures***, Vol. 42, (2005), 4220-4238.
15. Liew, K.M. and Chen, X.L., "Buckling of rectangular Mindlin plates subjected to partial in-plane edge loads using the radial point interpolation method", ***International Journal of Solids and Structures***, Vol. 41, (2004), 1677-1695.
16. Jana, P. and Bhaskar, K., "Stability analysis of simply-supported rectangular plates under non-uniform uniaxial compression using rigorous and approximate plane stress solutions", ***Thin-Walled Structures***, Vol. 44, (2006), 507-516.
17. Zhong, H. and Gu, C., "Buckling of symmetrical cross-ply composite rectangular plates under a linearly varying in-plane load", ***Composite Structures***, Vol. 80, (2007), 42-48.
18. Lopatin A.V, and Morozov E.V., "Buckling of the CCFF orthotropic rectangular plates under in-plane pure bending", ***Composite Structures***, Vol. 92, (2010), 1423-1431.
19. Panda, S.K. and Ramachandra, L.S., "Buckling of rectangular plates with various boundary conditions loaded by non-uniform inplane loads", ***International Journal of Mechanical Sciences*** , Vol. 52, (2010), 819-828.
20. Shanmugam, N.E. and Wang, C.M., Analysis and design of plated structures, Volume 1: Stability, CRC Press, Cambridge, (2006).
21. Bodaghi, M. and Saidi, A.R., "Buckling behavior of standing laminated Mindlin plates subjected to body force and vertical loading", ***Composite Structures***, Vol. 93, (2011), 538-547.
22. Naghdabadi, R. and Hosseini Kordkheili, S.A., "A finite element formulation for analysis of functionally graded plates and shells", ***Archive of Applied Mechanics***, Vol. 74, (2005), 375-386.
23. Saidi A.R., Jomehzadeh, E. and Atashipour, S.R., "Exact analytical solution for bending analysis of functionally graded annular sector plates", ***International Journal of Engineering Transactions A: Basics***, Vol. 22, (2009), 307-316.
24. Saidi A.R., Atashipour, S.R. and Jomehzadeh, E., "Exact elasticity solutions for thick-walled FG spherical pressure vessels with linearly and exponentially varying properties", ***International Journal of Engineering Transactions A: Basics***, Vol. 22, (2009), 405-416.
25. Nasr, A., Atashipour, S.R. and Fadaee M., "An elasticity solution for static analysis of functionally graded curved beam subjected to a shear force", ***International Journal of Engineering Transactions B: Applications***, Vol. 23, (2010), 169-178.
26. Fotros, F., Pashaei, M.H., Alashti, R.A. and Naei, M.H., "Effects of geometric nonlinearity on stress analysis in large amplitude vibration of thin circular functionally graded plates with rigid core", ***International Journal of Engineering Transactions A: Basics***, Vol. 24, (2011), 281-290.
27. Cheng, Z.Q. and Kitipornchai, S., "Membrane analogy of buckling and vibration of inhomogeneous plates", ***Journal of Engineering Mechanics***, Vol. 125, (1999), 1293-1297.
28. Wu, L., "Thermal buckling of a simply supported moderately thick rectangular FGM plate", ***Composite Structures*** , Vol. 64, (2004), 211-218.
29. Kazerouni, S.M., Saidi, A.R. and Mohammadi, M., "Buckling Analysis of Thin Functionally graded Rectangulare Plates with Two Opposite Edges Simply Supported", ***International Journal of Engineering Transactions B: Applications*** Vol. 23, (2010), 179-192.
30. Bodaghi M. and Saidi, A.R., "Thermoelastic buckling behavior of thick functionally graded rectangular plates", ***Archive of Applied Mechanics***, Vol. 81, (2011), 1555-1572.
31. Mohammadi, M., Saidi, A.R. and Jomehzadeh, E., "A novel analytical approach for buckling analysis of moderately thick functionally graded rectangular plates with two opposite edges simply supported", ***Proc. IMechE, Part C: Journal of Mechanical Engineering Science,*** Vol. 224, (2010), 1831-1841.
32. Morimoto, T., Tanigawa, Y. and Kawamura, R., "Thermal buckling of functionally graded rectangular plates subjected to partial heating", ***International Journal of Mechanical Sciences*** , Vol. 48, (2006), 926-937.
33. Abrate, S., "Functionally graded plates behave like homogeneous plates", ***Composites Part B***, Vol. 39, (2008), 151-158.
34. Zhang, D.G. and Zhou, Y.H., "A theoretical analysis of FGM thin plates based on physical neutral surface", ***Computational Materials Science***, Vol. 44, (2008), 716-720.
35. Prakash, T., Singha, M.K. and Ganapathi, M., "Influence of neutral surface position on the nonlinear stability behavior of functionally graded plates", ***Computational Mechanics***, Vol. 43, (2009), 341-350.
36. Saidi, A.R. and Jomehzadeh, E., "On analytical approach for the bending/stretching of linearly elastic functionally graded rectangular plates with two opposite edges simply supported", ***Proc. IMechE, Part C: Journal of Mechanical Engineering Science***, Vol. 223, (2009), 2009-2016.
37. Bodaghi, M. and Saidi, A.R., "Stability analysis of functionally graded rectangular plates under nonlinearly varying in-plane loading resting on elastic foundation", ***Archive of Applied Mechanics***, Vol. 81, (2011), 765-780.
38. Praveen, G.N. and Reddy, J.N., "Nonlinear transient thermoelastic analysis of functionally graded ceramic-metal plates", ***International Journal of Solids and Structures***, Vol. 35, (1998), 4457-4476.
39. Suresh, S. and Mortensen, A., Fundamentals of functionally graded materials, IOM Commun, Cambridge, (1998).
40. Brush, D.O. and Almroth, B.O., Buckling of bars, plates and shells, McGraw–Hill, New York, (1975).
41. Reddy, J.N., Theory and analysis of elastic plates, Taylor & Francis, Philadelphia, (1999).
42. Reddy, J.N., Energy principles and variational methods in applied mechanics, John Wiley, New York, (1984).
43. Wylie, C.R. and Barrett, L.C., Advanced engineering mathematics, McGraw-Hill, New York, (1951).